Isomer-driven polymerization, depolymerization, and reconstruction†

Herbert Wakefield IV,[a] Nicholas J. Fromel,[a] Jennifer Jiang,[a] Ilia Kevlishvili, [b]
Yunxin Yao,[c] Stephen L. Craig, [c] Heather J. Kulik [b] and Rebekka S. Klausen [*a]

We report that differences in ring strain enthalpy between *cis* and *trans* isomers of sila-cycloheptene provide a driving force for both polymerization and depolymerization *via* olefin metathesis. A need for new methods to reintroduce the low-strain isomer into the plastic economy inspired the development of a polymerization based on ring-opening/cross-metathesis step polymerization, which afforded perfect sequence control for an alternating copolymer. The chemical principles are a platform for achieving both efficient polymerization and depolymerization with high mass recovery in functional polymers.

Introduction

Chemical solutions to end-of-life management of post-consumer plastic waste are an emerging and urgent area of research.[1] Currently, less than 10% of plastic waste is mechanically recycled, instead ending in the landfill or incinerator (a linear plastic economy). In contrast to mechanical recycling, which can erode material properties due to changes in molecular weight characteristics arising from mechanical degradation, chemical recycling to monomer transforms plastic waste into feedstocks indistinguishable from petroleum-derived monomer, which can then reform pristine plastics (a more circular plastic economy).[2] Approaches to chemical recycling to monomer include comonomers or end groups in poly(methyl methacrylate) (PMMA) that trigger β-scission,[3–9] transesterification of poly(ethylene terephthalate),[10–13] self-immolative polymers,[14–16] and more.[17]

Olefin metathesis-based approaches to polymer deconstruction have been recently reviewed.[18] An attractive feature of this approach is that the polymer is stable until addition of the metathesis catalyst. Deconstruction can be a depolymerization process that returns the original starting monomer or a reaction yielding a different chemical building block.[19] Polymerization thermodynamics are critical:[20–23] if ring-opening metathesis polymerization (ROMP) is highly exother-

mic due to significant strain release, the reverse reaction (ring-closing metathesis (RCM) depolymerization) is challenging to effect. Chemical recycling to monomer by olefin metathesis was until recently limited to monomers with low-to-moderate ring strain,[22] while polymeric materials derived from higher strain monomers like norbornene and *cis*-cyclooctene[24] were not depolymerizable to monomer. Recently, structural modifications to *cis*-cyclooctene enabled chemical recycling to monomer by modulating ring-strain enthalpy (RSE) and polymerization–depolymerization thermodynamics.[21,25]

Exploiting the differences in RSE between *cis* and *trans* geometric isomers of the same cycloalkene has potential to broaden the scope of polymeric materials amenable to olefin metathesis polymerization–depolymerization, as shown by Wang *et al.* in a "closed-loop" photoisomerization-ROMP-RCM cycle of fused bicyclic cyclooctene monomers.[26] However, olefin photoisomerization has limitations: high-energy light is typically needed (*e.g.*, 254 nm) and the amount of *cis* isomer that can be converted to *trans* isomer is fundamentally limited by the photostationary *trans* : *cis* ratio. This means that not all the chemical matter recovered by depolymerization to the *cis*-isomer can reenter the cycle, highlighting the need for additional chemical methods to reintroduce the low-strain isomer into the plastic economy.

Herein, we demonstrate isomer-driven polymerization, depolymerization, and reconstruction of sila-cycloheptene by multiple olefin metathesis mechanisms. We recently reported the geometrically-selective synthesis of both the *cis* and *trans* isomers of sila-cycloheptene **1** in which *trans*-**1** was high strain (*ca.* 10 kcal mol⁻¹) and readily underwent ROMP.[27] **P1** is a novel example of a hybrid polymer incorporating both C and Si into the backbone. We showed *via* single molecule force spectroscopy that the Si incorporation into **P1** reduced single chain elasticity relative to all-carbon polymer backbones,

[a] Department of Chemistry, Johns Hopkins University, 3400 N. Charles St, Baltimore, MD, 21218, USA. E-mail: klausen@jhu.edu

[b] Department of Chemical Engineering, Massachusetts Institute of Technology, Cambridge, MA, 02139, USA

[c] Department of Chemistry, Duke University, Durham, NC, USA

†Electronic supplementary information (ESI) available: Supplemental figures, experimental procedures, NMR spectra, SEC elugrams. See DOI: https://doi.org/10.1039/d4py01281j

resulting in a softer, less stiff polymer strand, which was hypothesized to arise from force-induced changes in geometry and conformation at Si.[28] While *trans*-**1** was a good ROMP monomer, low strain *cis*-**1** (*ca.* 1–2 kcal mol^{-1}) did not polymerize. DFT calculations predicted that metathesis initiation is kinetically accessible for *cis*-**1**, but ROMP is endothermic.

We now report well-controlled ROMP of *trans*-**1** to afford a high molecular weight (>300 kg mol^{-1}) homopolymer **P1** that is stable in the absence of a metathesis initiator but undergoes 100% depolymerization to low-strain *cis*-**1** upon addition of an appropriate initiator (Fig. 1). To reuse the low-strain isomer, we hypothesized that ring-opened *cis*-**1** could be captured in a selective cross-metathesis reaction, resulting in a novel tandem ring-opening/cross-metathesis (RO-CM) olefin metathesis polymerization that is sequence-controlled. We show that recovered *cis*-**1** participates in RO-CM with butanediol diacrylate (BDA) to afford a perfectly alternating copolymer **P2**. This work demonstrates the ability of isomerism to drive novel polymer design, optimize reactivity, mass recovery, and reuse, as well as the role of Si for C replacement[29] in modulating monomer ring strain, polymerization thermodynamics, and polymer properties.

Results and discussion

Our initial efforts focused on identifying if molecular weight characteristics are important in depolymerization of **P1** as our initial publication reported a high molecular weight and high dispersity polymer (M_n = 62.6 kg mol^{-1}, M_w/M_n = 3.50) reflecting a multimodal sample containing both high molecular weight strands and oligomeric fragments.[27] The low molecular weight fraction included cyclic oligomers arising from ring-closing macrocyclization, which lack end groups and could complicate end-group selective initiation of depolymerization. To remove the lower molecular weight fraction, *trans*-**1** was polymerized to **P1**$_{5.03}$ as a polymodal sample then purified *via* recycling size exclusion chromatography (RSEC) and reprecipitated in methanol to afford narrow dispersity **P1**$_{1.23}$ (Fig. 2).
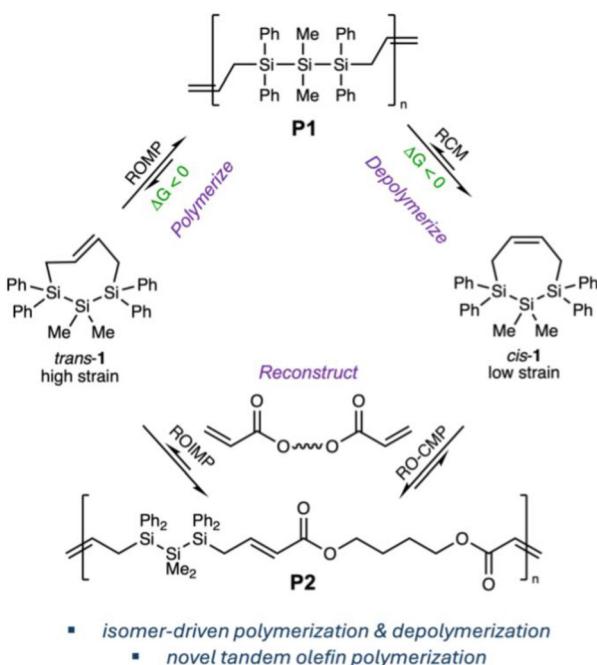
Unimodal **P1** can also be synthesized directly, as we have now also identified improved ROMP conditions. Hypothesizing that the formation of lower molecular weight oligomers arose from secondary metathesis reactions, we sought to rigorously purify *trans*-**1** by recrystallization to remove any olefinic contaminants from synthesis (*e.g.*, *trans*-1,4-dichlorobutene). With highly purified starting material and a much shorter reaction time of 10 minutes, **P1** was synthesized in high molecular weight and in a unimodal distribution (M_n = 92.9 kg mol^{-1}, M_w/M_n = 1.14, Scheme 1a).

Upon treatment of **P1**$_{1.23}$ with 1 mol% of the metathesis initiator **G1**, we observed after 16 hours by ^{1}H NMR spectroscopy the growth of peaks assigned to *cis*-**1** (55% conversion) with polymeric material remaining (Fig. 3). Consistent with chain transfer competing with depolymerization by RCM, multimodal **P1**$_{11.1}$ (containing residual oligomers) depolymerized in only 28% conversion under the same conditions (Fig. S2†).

Monitoring the depolymerization of **P1**$_{1.23}$ over time by SEC (Fig. 4 and Table 1), we observed a gradual decrease in the amount of **P1** and an increase in *cis*-**1**. Reisolation of **P1** at


Fig. 1 Intrinsic differences in ring strain of *trans*- and *cis*-**1** enable polymerization, depolymerization, and reconstruction by multiple olefin metathesis mechanisms. ROMP = ring-opening metathesis polymerization; RCM = ring-closing metathesis; ROIMP = ring-opening-insertion metathesis polymerization; RO-CMP = ring-opening/cross-metathesis polymerization.
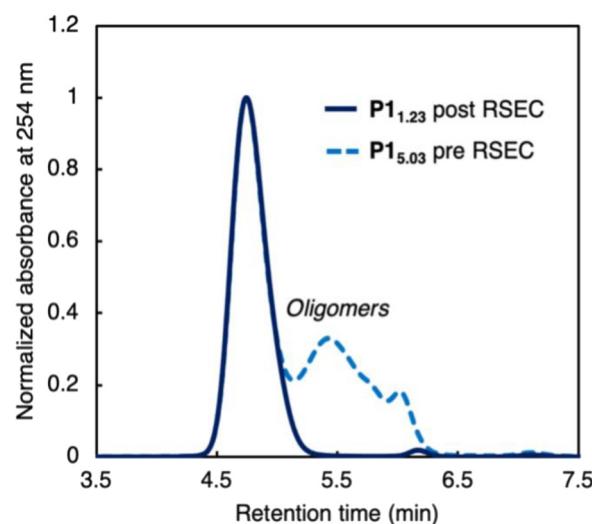
Fig. 2 Size exclusion chromatography (SEC) elugram of **P1** before (dashed) and after (solid) purification by recycling SEC, normalized to the largest molecular weight peak at 4.74 min ([**P1**] = 1.00 mg mL^{-1}, THF, RT) relative to polystyrene standards. **P1** (before RSEC) M_n = 2.03 kg mol^{-1}, M_w/M_n = 5.03. **P1** (after RSEC) M_n = 13.0 kg mol^{-1}, M_w/M_n = 1.23.

Published on 20 Ximoli 2024. Downloaded on 31/01/2026 3:06:02 PM.
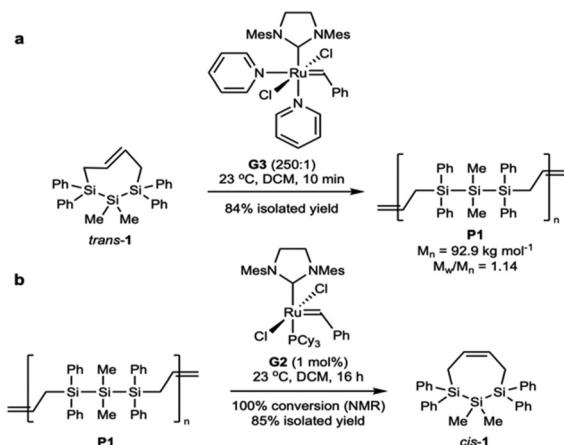
Scheme 1 (a) Optimized polymerization of *trans*-**1** to afford low dispersity **P1** and (b) optimized depolymerization of **P1** to afford *cis*-**1** in 85% yield.
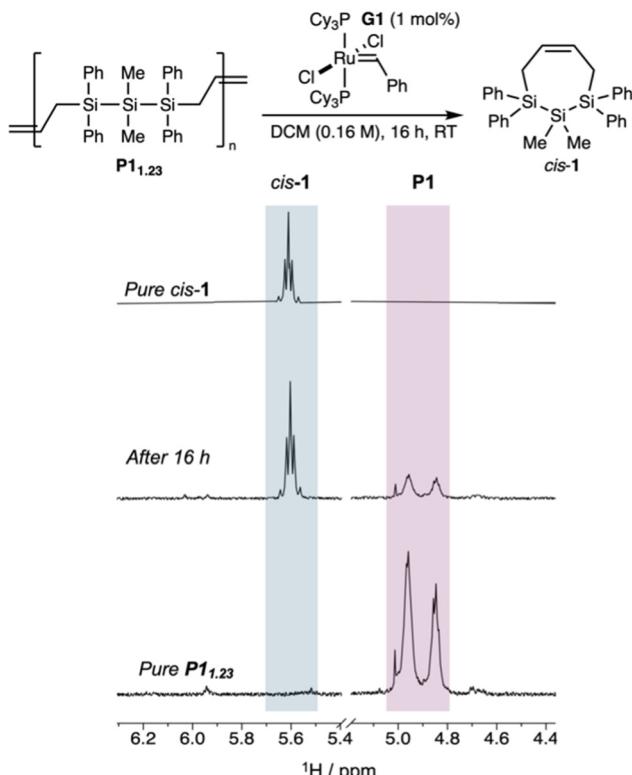
Fig. 3 Cropped ¹H NMR spectra of pure *cis*-**1** (top), after 16 hours of depolymerization (middle), and pure **P1**$_{1.23}$ (bottom) showing 55% depolymerization to *cis*-**1**.

each time point showed that M_n decreased from 11.9 kg mol⁻¹ to 6.92 kg mol⁻¹ while dispersity increased modestly from 1.30 to 1.81 (Table 1). Deconstruction at random internal sites would result in many more short oligomers and a much broader M_w/M_n than we observed here, suggesting a possible end-to-end depolymerization. At the same time, the modest increase in dispersity suggested that chain transfer might also
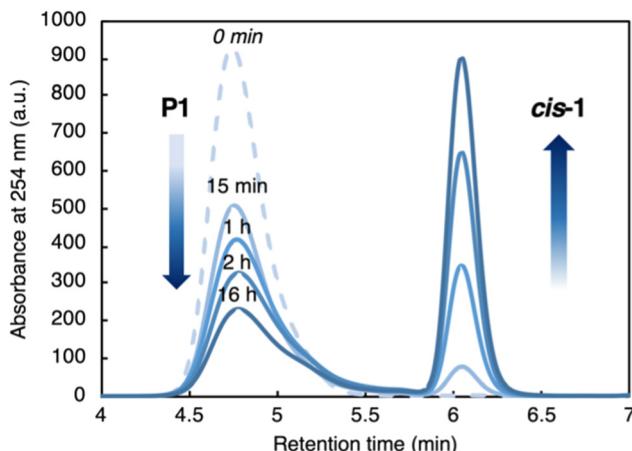
Fig. 4 SEC elugrams of recovered **P1** over time ([**P1**] = 0.75 mg mL⁻¹, THF, RT). See Table 1 for molecular weight characteristics of recovered **P1**.

Table 1 Molecular weight characteristics of recovered **P1** over time[a]

Reaction time	M_n[b] (kg mol⁻¹)	M_w/M_n[b]
0	11.9	1.30
15 min	9.55	1.51
1 h	8.0	1.68
2 h	7.12	1.79
16 h	6.92	1.81

[a] Depolymerization of **P1** performed at room temperature over 16 h with a concentration of 0.16 M in DCM and 1 mol% **G1**. [b] Determined by size exclusion chromatography relative to polystyrene standards at 254 nm (THF, [**P1**] = 0.75 mg mL⁻¹, 40 °C, 0.35 mL min⁻¹, 10 µL injection).

be occurring between strands, reducing the efficiency of depolymerization.

We investigated other metathesis initiators. While **G3** improved the depolymerization efficiency compared to **G1**, resulting in 86% depolymerization of **P1** to *cis*-**1**, the best conditions employed 1 mol% of **G2** and increased depolymerization efficiency to 100% conversion to *cis*-**1** (Table 2, entries 2

Table 2 Conversion of **P1** to *cis*-**1** under different conditions

Entry	M_w/M_n of starting **P1**	Cat.[a]	mol%	Temp. (°C)	% NMR yield[b] *cis*-**1**
1	1.23	**G1**	1	23	55
2	1.23	**G2**	1	23	100
3	2.13	**G2**	1	23	100 (85% isolate yield)
4	1.23	**G3**	1	23	86
5	11.1	**G1**	1	23	28
6	11.1	**G1**	3	23	38
7	11.1	**G1**	5	23	37
8	11.1	**G1**	1	50	36
9	8.61	**G2**	1	23	84

[a] Catalyst used for depolymerization. [b] Determined from the relative integration of the polymer olefinic protons and the olefinic protons of *cis*-**1**.

and 3), with no remaining high molecular weight polymer. In general, higher loadings of metathesis promoter and higher temperatures led to higher quantities of recovered *cis*-**1** (entries 5–7). Scaling up the best conditions, we were able to depolymerize 80 mg of **P1** to 100% conversion by ^{1}H NMR and with 85% isolated yield of *cis*-**1** (Table 2, entry 3). We hypothesize that the higher depolymerization efficiency with **G2** is related to its generally higher reactivity relative to **G1**[30] and employing **G2** instead of **G1** also increased the depolymerization efficiency of high dispersity material (compare entries 5 and 9).

Having identified the circumstances leading to complete depolymerization of **P1** to *cis*-**1**, we considered potential reuse scenarios for this low-strain cycloalkene. Entropy-driven ROMP can be an effective method for polymerization of low-strain cycloalkenes but requires high concentrations[31] and *cis*-**1** is a crystalline solid that is poorly soluble in CH_2Cl_2, $CHCl_3$ and other solvents (Table S1†). We considered alkene photoisomerization, but photochemical silylene extrusion[32] is possible for *cis*-**1**. In addition, the amount of *trans* isomer available from the *cis* isomer is limited by the photostationary *trans* : *cis* ratio.[33,34]

For these reasons, we sought an alternative polymerization method for *cis*-**1**. Prior calculated free energy profiles for initiation of *cis*- and *trans*-**1** ROMP with **G2**[27] indicated that *cis*-**1** is kinetically able to form a ring-opened, Ru-terminated structure similar to A (Fig. S3†).[35] While the reaction of A with *cis*-**1** to form a homopolymer *via* ROMP (a chain polymerization) is endothermic and not observed, we hypothesized that intermediate A could instead be captured in cross-metathesis. Reaction of A with a bifunctional Type 2 olefin B$_2$ would release the metathesis catalyst and difunctional molecule AB, which we anticipated would be a suitable step polymerization monomer[36] *via* selective cross-metathesis between terminal alkene and acrylate end groups.[37,38] Formation of the low energy α,β-unsaturated ester provides the driving force for ring-opening/cross-metathesis (RO-CM). While RO-CM is a tandem reaction extensively developed for small molecule synthesis,[39,40] it does not appear that RO-CM step polymerization has previously been reported. The polymerization by selective cross-metathesis of linear monomers with a terminal alkene and an acrylate supports our hypothesized mechanism.[37,38] It is plausible that both RO-CM and the reverse order of fundamental steps (cross metathesis/ring-opening, CM-RO) operate simultaneously, although CM-RO would require **G2** to react first with B$_2$ and then ring open *cis*-**1**[41,42] while the reaction of **G2** with acrylates is slower than with more activated olefins.

To test the hypothesized RO-CM reactivity, we carried out two small molecule studies in which we reacted *cis*-**1** with 1-hexene (Type 1 olefin) or methyl acrylate (Type 2 olefin). With 1-hexene, we only observed the formation of the homodimerization product 4-decene and residual *cis*-**1** (Fig. S4†). But in the presence of excess methyl acrylate, the ring-opened structure **2** was isolated in 61% yield after purification by silica gel chromatography (Scheme 2). The RO-CM product **2** has
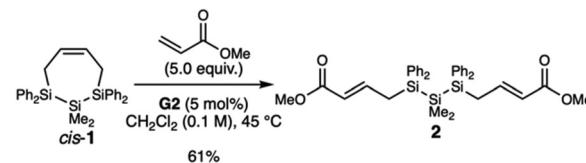
Scheme 2 Model reaction for ring opening–cross metathesis (RO-CM) of *cis*-**1** and methyl acrylate.

exclusively the *trans* olefin geometry, as determined by the coupling constants of the olefinic peaks δ 6.81 ($J_{1H–1H}$ = 15.5 Hz) and δ 5.39 ($J_{1H–1H}$ = 15.4 Hz) (Fig. S5†).

Expanding from molecular RO-CM, we then investigated the RO-CM step polymerization of *cis*-**1** and 1,4-butanediol diacrylate (BDA) (Fig. 5b). We observed 91% consumption of *cis*-**1** within 4.5 hours. By precipitation from hexanes, we obtained polymer **P2** (M_n = 3.31 kg mol^{-1}, M_w/M_n = 1.87). Structural characterization supported incorporation of both monomers. ATR-IR spectroscopy (Fig. S5†) indicated the presence of an α,β-unsaturated carbonyl at 1706 cm^{-1}, as well as a SiMe functional group at 1257 cm^{-1}.

Since *cis*-**1** is a poor ROMP monomer and BDA is a poor ADMET monomer, RO-CM predicts an alternating copolymer due to faster crosspolymerization than homopolymerization. Structural characterization supported assignment of **P2** to a highly alternating polymer (>99% alteration) based on ^{1}H NMR spectroscopy (Fig. 6) in which neither the singlet consistent with a fumarate resonance nor the lower field resonances of a diallyl silane were observed. The major peaks were assigned to the alternating copolymer and were consistent with an (*E*)-geometry. Resonances consistent with both acrylate and styrenic end groups were identified and full details of copolymer structural characterization are reported in the ESI.† We note that **P2** can itself be deconstructed at end of life by ester hydrolysis.

To understand the impact of BDA incorporation onto the properties of a hybrid carbosilane polymer, we measured the glass transition temperature (T_g) of **P2**. While the homopolymer **P1** exhibits a glass transition temperature a little above room temperature (*ca.* 35 °C), the alternating copolymer **P2** had a T_g *ca.* 13 °C. The lower T_g may reflect the additional incorporation of the flexible butane chain and a lower overall aromatic side chain content. In recent years, the role of sequence control has emerged as a tactic for modulating the glass transition temperature of a copolymer.[43] The onset of thermal decomposition occurred at *ca.* 300 °C, consistent with other Si–Si containing polymers.[27,44]

This tandem ring-opening and selective cross-metathesis polymerization has the advantage of very high sequence control, a grand challenge in polymer synthesis.[45,46] The copolymerization of cycloalkenes and α,ω-diene monomers related to Type 1 olefins is known, but not sequence controlled.[47,48] Alternating copolymerization by olefin metathesis has been reported with cyclohexene and electron-poor strained cycloalkenes (*e.g.*, cyclobutenecarboxamide).[49] The most similar reac-
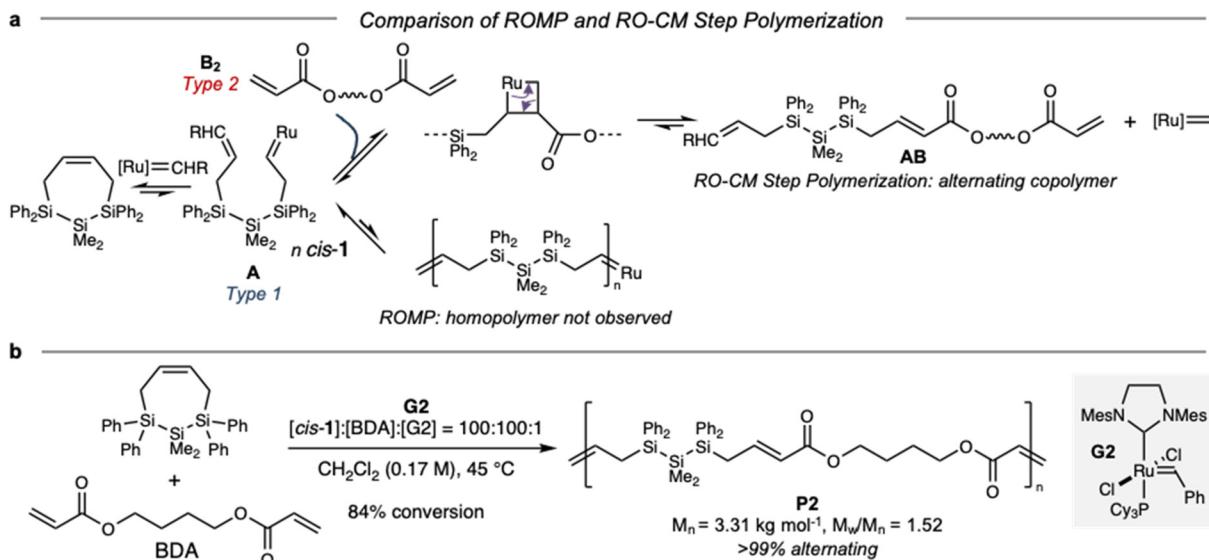
Fig. 5 (a) Proposed mechanism for ring-opening/cross-metathesis step polymerization yielding highly alternating copolymers. (b) Synthesis of **P2** *via* RO-CM step polymerization.
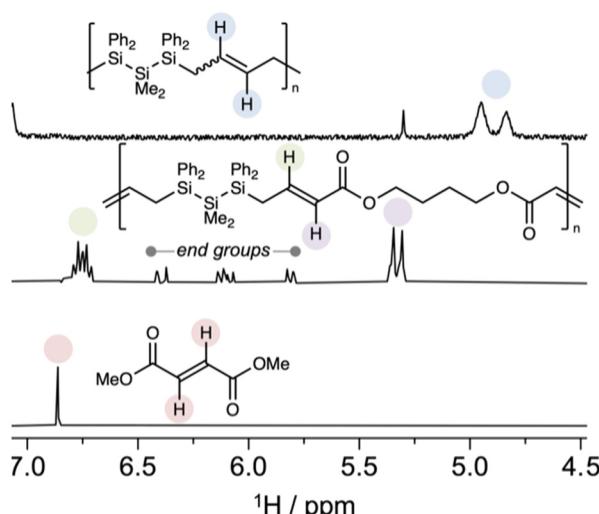

Fig. 6 Cropped ^{1}H NMR spectra (CDCl₃, 400 MHz) comparing the olefinic regions of **P1** (top), **P2** (middle), and dimethyl fumarate (bottom). There is no evidence of signals consistent with consecutive homopolymerization repeat units, supporting a highly alternant copolymer microstructure.

tion to ours is ring-opening-insertion metathesis polymerization (ROIMP). ROIMP is the copolymerization of cycloalkenes and diacrylates to yield highly alternant copolymers,[50–53] but ROIMP proceeds by a distinctly different mechanism involving first rapid cycloalkene ROMP (*e.g.*, *cis*-cyclooctene), followed by insertion of BDA or other diacrylate into the homopolymer by a slower secondary metathesis process.

In the current work, the lack of *cis*-**1** homopolymerization and the well-precedented slow rate of acrylate dimerization are not consistent with a ROIMP mechanism involving insertion

of a second monomer into a homopolymer. A series of control experiments suggested that *cis*-**1**/BDA RO-CM copolymerization proceeds by a mechanism that is distinct from ROIMP and that these differences result in meaningful impacts on polymer microstructure *e.g.*, sequence control.

First, we evaluated the reactivity of *trans*-**1** and BDA under the same conditions employed for *cis*-**1**. We observed a mixture that consisted predominantly of **P1** and unreacted BDA, with evidence of smaller amounts of dimeric BDA and **P2** (Fig. S6†). This is distinctly different from the outcome with *cis*-**1**, where no homopolymers were observed, and is consistent with high strain *trans*-**1** being suitable for ROIMP while low strain *cis*-**1** reacts *via* RO-CM step polymerization.

Second, we noted that Choi and Grubbs reported that polycyclooctene could be used directly as a substrate for ROIMP, supporting the hypothesis that the homopolymer is an intermediate. If ROIMP was operative for the copolymerization of *cis*-**1**/BDA, **P1** should react with BDA to yield **P2**. However, the reaction between homopolymer **P1** and BDA afforded only residual **P1** and small quantities of the BDA dimer/oligomer, but no spectroscopic evidence of either *cis*-**1** or **P2** (Fig. S10†).

Third, a consequence of the ROIMP mechanism is that extended homopolycycloalkene segments were found at early time points (*e.g.*, 20 min).50 For *cis*-**1**/BDA copolymerization, high alternation of 82.0% was observed after 15 minutes (Fig. S11†). This points to the very high selectivity for cross-metathesis rather than homopolymerization.

Conclusions

The isomer-driven metathesis reactivity reported herein highlights how subtle differences in structure, thermodynamics, and kinetics can be exploited in the well-controlled, serial

polymerization/depolymerization/reconstruction pathways. Only the *trans* isomer of sila-cycloheptene **1** undergoes ROMP by chain polymerization, driven by strain release. The reverse ring-closing metathesis reaction yields only the low-strain *cis* isomer of **1**, driven by the entropic benefit of depolymerization, and leading to 100% selectivity for a single product and 100% conversion in chemical recycling. The use of cycloalkene geometric isomerism to affect the position of polymer thermodynamics is recently emerging, building onto the use of *cis*/*trans* relative configuration at tetrahedral stereoegenic centers.[54,55] We reintroduce *cis*-**1** into polymeric materials by a novel tandem olefin metathesis pathway involving ring-opening/cross-metathesis step polymerization. Tandem olefin metathesis reactions remain rare in macromolecular synthesis due to poor control,[51] but herein we achieved perfect selectivity for the cross-metathesis reaction and obtained a highly alternant copolymer from *cis*-**1** and the diacrylate BDA. The resulting polymer was fully characterized by ATR-IR, ^{1}H, ^{13}C, ^{29}Si, COSY, and HSQC NMR spectroscopy to determine polymer microstructure.

That a 7-membered ring can switch from a high to a low-strain reactivity manifold is enabled not only by controlling olefin geometry, but also by the ability of Si for C replacement to modulate ring conformation and geometry (*trans*-cycloheptene is unstable >−40 °C).[56] The work described herein showcases that subtle structural modifications can have dramatic effects on chemical reactivity relevant to polymer end-of-life management.

Data availability

The data supporting this article have been included as part of the ESI.†

Conflicts of interest

There are no conflicts to declare.

Acknowledgements

References

1 D. E. Fagnani, J. L. Tami, G. Copley, M. N. Clemons, Y. D. Y. L. Getzler and A. J. McNeil, *ACS Macro Lett.*, 2021, **10**, 41–53.

2 G. W. Coates and Y. D. Y. L. Getzler, *Nat. Rev. Mater.*, 2020, **5**, 501–516.

3 J. B. Young, R. W. Hughes, A. M. Tamura, L. S. Bailey, K. A. Stewart and B. S. Sumerlin, *Chem*, 2023, **9**, 2669–2682.

4 R. W. Hughes, M. E. Lott, I. S. Zastrow, J. B. Young, T. Maity and B. S. Sumerlin, *J. Am. Chem. Soc.*, 2024, **146**, 6217–6224.

5 M. R. Martinez, S. Dadashi-Silab, F. Lorandi, Y. Zhao and K. Matyjaszewski, *Macromolecules*, 2021, **54**, 5526–5538.

6 H. S. Wang, N. P. Truong, Z. Pei, M. L. Coote and A. Anastasaki, *J. Am. Chem. Soc.*, 2022, **144**, 4678–4684.

7 M. T. Chin, T. Yang, K. P. Quirion, C. Lian, P. Liu, J. He and T. Diao, *J. Am. Chem. Soc.*, 2024, **146**, 5786–5792.

8 R. Whitfield, G. R. Jones, N. P. Truong, L. E. Manring and A. Anastasaki, *Angew. Chem., Int. Ed.*, 2023, **62**, e202309116.

9 V. Bellotti, K. Parkatzidis, H. S. Wang, N. De Alwis Watuthanthrige, M. Orfano, A. Monguzzi, N. P. Truong, R. Simonutti and A. Anastasaki, *Polym. Chem.*, 2023, **14**, 253–258.

10 N. George and T. Kurian, *Ind. Eng. Chem. Res.*, 2014, **53**, 14185–14198.

11 H. Tang, N. Li, G. Li, A. Wang, Y. Cong, G. Xu, X. Wang and T. Zhang, *Green Chem.*, 2019, **21**, 2709–2719.

12 M. Wang, Y. Li, L. Zheng, T. Hu, M. Yan and C. Wu, *Polym. Chem.*, 2024, **15**, 585–608.

13 K. R. Delle Chiaie, F. R. McMahon, E. J. Williams, M. J. Price and A. P. Dove, *Polym. Chem.*, 2020, **11**, 1450–1453.

14 J. P. Lutz, O. Davydovich, M. D. Hannigan, J. S. Moore, P. M. Zimmerman and A. J. McNeil, *J. Am. Chem. Soc.*, 2019, **141**, 14544–14548.

15 J. Yuan, G. J. Giardino and J. Niu, *Angew. Chem., Int. Ed.*, 2021, **60**, 24800–24805.

16 M. Hansen-Felby, A. Sommerfeldt, M. L. Henriksen, S. U. Pedersen and K. Daasbjerg, *Polym. Chem.*, 2022, **13**, 85–90.

17 C. F. Gallin, W. Lee and J. A. Byers, *Angew. Chem., Int. Ed.*, 2023, **62**, e202303762.

18 D. Sathe, S. Yoon, Z. Wang, H. Chen and J. Wang, *Chem. Rev.*, 2024, **124**, 7007–7044.

19 R. J. Conk, S. Hanna, J. X. Shi, J. Yang, N. R. Ciccia, L. Qi, B. J. Bloomer, S. Heuvel, T. Wills, J. Su, A. T. Bell and J. F. Hartwig, *Science*, 2022, **377**, 1561–1566.

20 P. Olsén, K. Odelius and A.-C. Albertsson, *Biomacromolecules*, 2016, **17**, 699–709.

21 J. Zhou, D. Sathe and J. Wang, *J. Am. Chem. Soc.*, 2022, **144**, 928–934.

22 W. J. Neary and J. G. Kennemur, *ACS Macro Lett.*, 2019, **8**, 46–56.

23 D. Zhang, X. Wang, Z. Zhang and N. Hadjichristidis, *Angew. Chem., Int. Ed.*, 2024, **63**, e202402233.

24 H. Martinez, N. Ren, M. E. Matta and M. A. Hillmyer, *Polym. Chem.*, 2014, **5**, 3507.

25 D. Sathe, J. Zhou, H. Chen, H.-W. Su, W. Xie, T.-G. Hsu, B. R. Schrage, T. Smith, C. J. Ziegler and J. Wang, *Nat. Chem.*, 2021, **13**, 743–750.

26 H. Chen, Z. Shi, T. Hsu and J. Wang, *Angew. Chem., Int. Ed.*, 2021, **60**, 25493–25498.

27 H. Wakefield, I. Kevlishvili, K. E. Wentz, Y. Yao, T. B. Kouznetsova, S. J. Melvin, E. G. Ambrosius, A. Herzog-Arbeitman, M. A. Siegler, J. A. Johnson, S. L. Craig, H. J. Kulik and R. S. Klausen, *J. Am. Chem. Soc.*, 2023, **145**, 10187–10196.

28 K. E. Wentz, Y. Yao, I. Kevlishvili, T. B. Kouznetsova, B. A. Mediavilla, H. J. Kulik, S. L. Craig and R. S. Klausen, *Macromolecules*, 2023, **56**, 6776–6782.

29 H. Wakefield, S. J. Melvin, J. Jiang, I. Kevlishvili, M. A. Siegler, S. L. Craig, H. J. Kulik and R. S. Klausen, *Chem. Commun.*, 2024, **60**, 4842–4845.

30 M. Scholl, S. Ding, C. W. Lee and R. H. Grubbs, *Org. Lett.*, 1999, **1**, 953–956.

31 A. K. Pearce, J. C. Foster and R. K. O'Reilly, *J. Polym. Sci., Part A:Polym. Chem.*, 2019, **57**, 1621–1634.

32 A. G. Moiseev and W. J. Leigh, *J. Am. Chem. Soc.*, 2006, **128**, 14442–14443.

33 G. S. Hammond and J. Saltiel, *J. Am. Chem. Soc.*, 1962, **84**, 4983–4984.

34 Y. Inoue, T. Kobata and T. Hakushi, *J. Phys. Chem.*, 1985, **89**, 1973–1976.

35 A. K. Chatterjee, T.-L. Choi, D. P. Sanders and R. H. Grubbs, *J. Am. Chem. Soc.*, 2003, **125**, 11360–11370.

36 G. Odian, *Principles of polymerization*, J. Wiley & sons, Hoboken (N.J.), 4th edn, 2004.

37 L. Montero De Espinosa and M. A. R. Meier, *Chem. Commun.*, 2011, **47**, 1908–1910.

38 I. A. Gorodetskaya, T.-L. Choi and R. H. Grubbs, *J. Am. Chem. Soc.*, 2007, **129**, 12672–12673.

39 J. P. Morgan, C. Morrill and R. H. Grubbs, *Org. Lett.*, 2002, **4**, 67–70.

40 M. L. Randall, J. A. Tallarico and M. L. Snapper, *J. Am. Chem. Soc.*, 1995, **117**, 9610–9611.

41 M. Ulman, T. R. Belderrain and R. H. Grubbs, *Tetrahedron Lett.*, 2000, **41**, 4689–4693.

42 T.-L. Choi, C. W. Lee, A. K. Chatterjee and R. H. Grubbs, *J. Am. Chem. Soc.*, 2001, **123**, 10417–10418.

43 W. F. Drayer and D. S. Simmons, *Macromolecules*, 2022, **55**, 5926–5937.

44 Q. Jiang, S. Wong and R. S. Klausen, *Polym. Chem.*, 2021, **12**, 4785–4794.

45 J.-F. Lutz, M. Ouchi, D. R. Liu and M. Sawamoto, *Science*, 2013, **341**, 1238149.

46 Z. Li and Z. Li, in *Sequence–Controlled Polymers*, ed. J. Lutz, Wiley, 1st edn, 2018, pp. 349–377.

47 G. Si and C. Chen, *Nat. Synth.*, 2022, **1**, 956–966.

48 G. Si, Z. Wang, C. Zou and C. Chen, *CCS Chem.*, 2024, 1–10.

49 K. A. Parker and N. S. Sampson, *Acc. Chem. Res.*, 2016, **49**, 408–417.

50 T.-L. Choi, I. M. Rutenberg and R. H. Grubbs, *Angew. Chem.*, 2002, **114**, 3995–3997.

51 H.-K. Lee, K.-T. Bang, A. Hess, R. H. Grubbs and T.-L. Choi, *J. Am. Chem. Soc.*, 2015, **137**, 9262–9265.

52 C. Chauveau, S. Fouquay, G. Michaud, F. Simon, J.-F. Carpentier and S. M. Guillaume, *ACS Appl. Polym. Mater.*, 2019, **1**, 1540–1546.

53 C. Chauveau, S. Fouquay, G. Michaud, F. Simon, J.-F. Carpentier and S. M. Guillaume, *ACS Appl. Polym. Mater.*, 2020, **2**, 5135–5146.

54 S.-Y. Shan, W. Zhang, Q. Cao, Y.-C. Ye, Z. Cai and J.-B. Zhu, *Polym. Chem.*, 2024, **15**, 1070–1076.

55 M. L. Smith, T. M. McGuire, A. Buchard and C. K. Williams, *ACS Catal.*, 2023, **13**, 15770–15778.

56 M. E. Squillacote, J. DeFellipis and Q. Shu, *J. Am. Chem. Soc.*, 2005, **127**, 15983–15988.